

Elsevier Editorial System(tm) for Journal of Parallel and Distributed Computing  
Manuscript Draft

Manuscript Number: JPDC-13-56R1

Title: Parameter Variation Sensing and Estimation in Nanoscale Fabrics

Article Type: Special Issue: Nanotechnology

Keywords: Parameter Variation; Random Variation; On-chip Variation Sensor; NASIC; Nanowire Fabric

Corresponding Author: Mr. Jianfeng Zhang, M.D.

Corresponding Author's Institution: University of Massachusetts Amherst

First Author: Jianfeng Zhang, M.D.

Order of Authors: Jianfeng Zhang, M.D.; Mostafizur Rahman; Pritish Narayanan; Santosh Khasanvis;  
Csaba A Moritz, Professor

Abstract: Parameter variations introduced by manufacturing imprecision are becoming more influential on circuit performance. This is especially the case in emerging nanoscale computing fabrics due to unconventional manufacturing steps and aggressive scaling. On-chip variation sensors are gaining in importance since post-fabrication compensation techniques can be employed. In estimation with on-chip variation sensors, however, random variations are masked because of well-known averaging effects during measurements. We propose a new on-chip sensor for nanoscale computing fabrics to estimate random variations in physical parameters. We show detailed estimation methodology and validate it with Monte Carlo simulations. The results show the sensor estimation error to be 8% on average and 12.7% in worst case. In comparison to the well-known ring-oscillator based approach developed for CMOS, the estimation accuracy is 1.6X better and requires 40X less devices in on-chip sensors.

Suggested Reviewers:

Opposed Reviewers:

Jul. 27, 2013

Re: Submit a New Manuscript

**“Parameter Variation Sensing and Estimation in Nanoscale Fabrics”**

By Jianfeng Zhang, Mostafizur Rahman, Pritish Narayanan, Santosh Khasanvis  
and C. Andras Moritz

Dear Editor for JPDC,

I am writing to submit our manuscript entitled, “Parameter Variation Sensing and Estimation in Nanoscale Fabrics,” for publication consideration in “Special Issue of Journal of Parallel and Distributed Computing: Computing with Future Nanotechnology”. In this paper, we propose a novel sensor design for random variation estimation in emerging nanoscale computing fabrics, and show detailed variation sensing methodology, and evaluation results.

As transistors’ feature sizes shrink into deep nanoscale, random parameter variations due to manufacturing imprecision are gaining their influence on circuit performance, especially for emerging nanoscale computing fabrics where the extent of variation in physical parameters (e.g., channel doping density, gate oxide thickness) can be very high. These random parameter variations can lead to performance deterioration and yield loss in the integrated circuits. In order to address these variations, on-chip variation sensors are gaining their importance with post-fabrication compensation techniques being introduced. However, CMOS variation sensing approaches with ring-oscillators (RO) might not be suitable for emerging nanoscale fabrics, since the influence of random parameter variations are averaged out in RO frequency based measurements, and the area overhead for such sensors is very high.

In this paper, a novel variation sensor design is proposed, which can estimate random variations in physical parameters (e.g., channel doping density, source-drain doping density) based on the measured fall and rise times from sensor circuits. The detailed estimation methodology is presented and validated through HSPICE Monte Carlo simulations. The simulated results show the estimation error to be 12.7% in worst case and 8% on average. In comparison to the well-known ring-oscillator based approach developed for CMOS, the estimation accuracy is 1.6X better and requires 40X less devices in on-chip sensors.

This manuscript describes original work and is not under consideration by any other journal. All authors approved the manuscript and this submission.

Thank you for receiving our manuscript and considering it for review. We appreciate your time and look forward to your response.

Sincerely,  
Jianfeng Zhang

Department of Electrical and Computer Engineering at University of Massachusetts Amherst,  
Amherst MA 01003 USA  
Email: zljmfy@gmail.com

Dear reviewers,

Answers to your comments are listed below.

1. **Question:** There is no explanation on how the rise time and the fall time are measured on-chip. What circuit is used? It is likely that the measurement circuit introduces its self variability that has to be taken into account.

**Answer:** There are some existing approaches for measuring fall and rise times during run time. One paper has been cited in the revised version, which shows one on-chip circuit system to measure fall and rise times. Since these circuits are designed in CMOS, the variations in these circuits are much smaller compared with variations in our sensors designed in nanoscale fabrics. As a result, variations in these circuits will not affect the estimation accuracy very much.

2. **Question:** All the figures (especially the one that described algorithms) are too small and their resolution is too low, not readable. Please enlarge the figures and increase their resolution.

**Answer:** The resolution of all figures has been improved.

3. **Question:** The reason why function 'f', 'g', 'h' and 'p' are considered as polynomial should be briefly justified.

**Answer:** Since functions 'f', 'g', 'h' and 'p' are populated by curve fitting and our objective is to fit the sampled data with the simplest functions, polynomial functions are chosen.

4. **Question:** Section 5 Results: Why did you choose different polynome order (3 or 5). Does it result of a previous mathematical analyze or did you proceed through try / error?

**Answer:** Based on the accuracy of curve fitting, 3rd and 5th order polynomial functions fit the sampled data best.

5. **Question:** Page 6, paragraph 3: "Since each of our parameters is mainly dependent on a separate process step, we assume ..." Basically, because CD/SDD/U are independent factors, you decompose them into sum of each factor. Is it possible they are independent but the total effect is not addition of each, e.g., multiplication instead?

**Answer:** Because random variations in these physical parameters come from different manufacturing steps, we made this assumption. Interdependencies among these physical parameters would introduce cross-terms in the estimation equations that only increase the complexity of computation, but our approach still works.

## Highlights (for review)

- A novel variation sensor for nanoscale computing fabrics is proposed.
- Detailed on-chip random parameter variation sensing methodology is presented.
- An evaluation framework based on HSPICE Monte Carlo simulations is presented.
- Sensor accuracy was found to be 8% on average and 12.7% in the worst case.

# Parameter Variation Sensing and Estimation in Nanoscale Fabrics

Jianfeng Zhang, Mostafizur Rahman, Pritish Narayanan, Santosh Khasanvis and C. Andras Moritz  
Department of Electrical and Computer Engineering at University of Massachusetts Amherst  
Amherst MA 01003 USA  
Phone: 413-461-8945. Email: [zljmfy@gmail.com](mailto:zljmfy@gmail.com)

*Abstract*—Parameter variations introduced by manufacturing imprecision are becoming more influential on circuit performance. This is especially the case in emerging nanoscale computing fabrics due to unconventional manufacturing steps and aggressive scaling. On-chip variation sensors are gaining in importance since post-fabrication compensation techniques can be employed. In estimation with on-chip variation sensors, however, random variations are masked because of well-known averaging effects during measurements. We propose a new on-chip sensor for nanoscale computing fabrics to estimate random variations in physical parameters. We show detailed estimation methodology and validate it with Monte Carlo simulations. The results show the sensor estimation error to be 8% on average and 12.7% in worst case. In comparison to the well-known ring-oscillator based approach developed for CMOS, the estimation accuracy is 1.6X better and requires 40X less devices in on-chip sensors.

*Keywords:* Parameter Variation, Random Variation, On-chip Variation Sensor, NASIC, Nanowire Fabric

## 1. Introduction

Emerging nanoscale computing systems have been proposed as an alternative to scaled CMOS with potential performance and density benefits. These nanoscale computing systems are based on novel nanostructures, such as nanowires [1], [2], carbon nanotubes [3], graphene [4], [5], magneto electric devices [6], [7], [8], etc. Their manufacturing approaches incorporate unconventional (e.g., self-assembly, nano-imprint) and conventional (e.g., deposition, etching, and lithography) process steps. As their feature sizes shrink into deep nanoscale, the manufacturing process may cause a significant level of variations in physical parameters. For example, during dopant implantation, there exists some randomness in the distribution of dopants, which can result in the fluctuation of total number of dopants in a specified region. These variations could potentially lead to performance deterioration such as timing errors and consequently yield loss.

Parameter variations are traditionally addressed pre-fabrication by circuit design, often targeting worst-case variation scenarios. However, this pre-fabrication approach is pessimistic and performance benefits can be lost especially for nanoscale fabrics where the extent of variability can be high. Alternatively, if parameter variations could be estimated post-fabrication, some compensation techniques, such as redundant intermediate bitslices [9] and dynamic fine-grain body biasing [10], could be used to adjust circuit timing and reduce leakage power during run-time, leading to area and performance benefits.

Conventional variation estimation methods [11], [12] assume that large circuits are not affected by random variations because of an averaging effect; i.e., the influence of random variations is assumed to be nullified if the number of transistors in the critical path is large [13]. However, at nanoscale the impact of random variations cannot be neglected, since the influence is non-linear on circuit performance. For example, in [14] it was shown that there exists non-linear relationship between the on-current of devices and random variations in certain parameters (e.g., channel doping, source-drain doping and underlap). The system level performance was shown to degrade considerably as a result of random variations, with 67% of simulated chips operating at less than their nominal frequency [14]. Therefore, we believe that in order to estimate parameter variations accurately, random variations should be explicitly taken into consideration.

In this paper we propose a novel on-chip sensor design for quantifying the statistical distribution and impact of random variations in physical parameters for the Nanoscale Application Specific Integrated Circuits (NASICs) fabric [15], [16], [17], [18], [19]. The proposed sensor can estimate the statistical distribution of random variations in physical parameters in a chip from its own variations. This is also possible because NASICs rely on a uniform array-based structure with identical devices and no arbitrary sizing or doping; consequently, this implies that sensor circuits designed with the same devices and logic styles can represent the fabric as a whole. This sensor design and methodology is also directly applicable to the Nanoscale 3-D Application Specific Integrated Circuits ( $N^3$ ASICs) [20], [21], and the methodology can be extended to other regular nanoscale fabrics in general.

We first explain the principles of sensor design, and describe the methodology for variability sensing. In our sensor, signal fall and rise times are used to extract the statistical distribution of random variations in different physical parameters. These fall and rise times can be easily and accurately measured by some existing approaches as shown in [22]. Further, we present a methodology for evaluating and validating this sensor design using Monte Carlo circuit simulations. The simulation results obtained from 150 variation sensors show that the relative error between the injected and estimated standard deviation of physical parameters is 12.7% in the worst-case and 8% on average scenarios. Compared with the ring-oscillator (RO) based sensor design in CMOS technology shown in [23], the worst-case estimation error is improved by 1.6X, and the total number of devices required in on-chip sensors is reduced by 40X.

The rest of this paper is organized as follows: Section 2 briefly presents the NASIC fabric with emphasis on physical parameter variation; Section 3 illustrates the new sensor design and discusses the theoretical framework for estimating the distribution of random variations in physical parameters; Section 4 describes the Monte Carlo simulation methodology for evaluating the sensor design; simulated results for the sensor accuracy are shown in Section 5; and Section 6 concludes the paper.

## 2. NASICs Fabric Overview

Nanoscale Application Specific Integrated Circuits (NASICs) is a nanoscale computational fabric that relies on 2-D grids of semiconductor nanowires with crossed nanowire field-effect transistors (xnfETs) at certain crosspoints (Fig. 1). In this fabric, in order to ease manufacturing requirements, a regular grid layout is used where all transistors on the crosspoints are identical with no arbitrary doping or sizing requirements. This semiconductor nanowire grid includes some peripheral micro wires to carry  $VDD$ ,  $GND$  and control signals. Dynamic circuit styles without the requirement of complementary devices or arbitrary placement/sizing are used for logic implementation. Several extensions exist to NASICs and there are other circuit styles also proposed but the approach for variability estimation applies across all of them.

The dynamic circuit style and xnfET structure are shown in Fig. 2 and Fig. 3. Fig. 2 shows an  $N$ -input dynamic NAND gate with xnfETs as active devices. The *pre* and *eva* signals in this NAND gate are used to precharge and discharge the output (*out*), respectively, depending on inputs ( $in_1, in_2, \dots, in_N$ ). Multiple stages of logic can be achieved by cascading multiple such dynamic NAND gates. The proposed sensor follows the same dynamic circuit style.

The assumed xnfET device operating principle in this paper is similar to that of inversion mode devices; the current through the channel nanowire is modulated by the potential applied on the orthogonal gate. Sources of random variations in this

xnwFET structure include channel doping (*CD*), source-drain doping (*SDD*) and underlap (*U*). In this paper, random variations in *CD*, *SDD* and *U* are considered; systematic variation (e.g., channel/gate diameter, gate/bottom oxide thickness) estimation was shown in our previous paper [24].

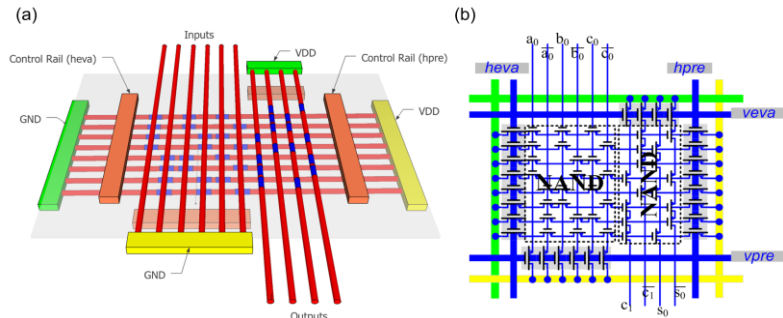


Fig.1 Nanoscale Application Specific Integrated Circuits with regular semiconductor nanowire grids, xnwFET devices and peripheral microscale control a) 3-D fabric view b) circuit schematic

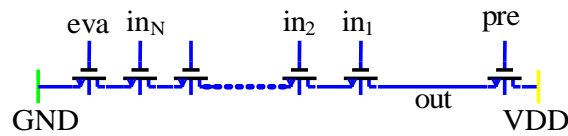


Fig.2 *N*-input NASIC dynamic NAND gate

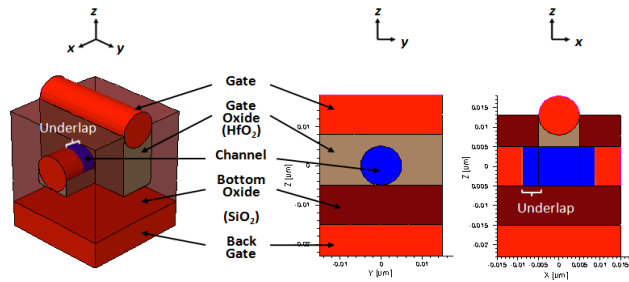


Fig.3 n-type xnwFET device structure with orthogonal gate and channel nanowires

### 3. On-chip Variation Sensor Design

A key motivation for a novel on-chip sensor design is that a conventional RO-based sensor design may be unsuitable for random-variation estimation in these emerging fabrics. This is mainly because: (i) the RO frequency averages the parameters of transistors in all stages and cannot thus accurately represent the characterization of random variations on individual devices; and (ii) RO-based sensors occupy a large fraction of chip area since the number of RO stages required is typically more than 100 for each sensor.

In this section, we discuss a new on-chip sensor design in the context of the NASIC fabric. The sensor can be used to estimate the statistical distribution of random variation in physical parameters based on the measured fall time (*I-to-0* transitions) and rise time (*0-to-I* transitions) from the sensor circuit.

Fig. 4a shows the new sensor circuit with only two xnwFETs. Two control signals *pre* and *eva* are used. When *pre* signal is ‘1’ and *eva* signal is ‘0’, the output is charged to ‘1’ at first, and then discharged to ‘0’ by inverting *pre* and *eva* signals. A load capacitance connected to output is designed to be much larger than device parasitics related capacitances. There are two reasons for using a large capacitance: 1) this load capacitance can amplify fall and rise times of the output, making them easier to

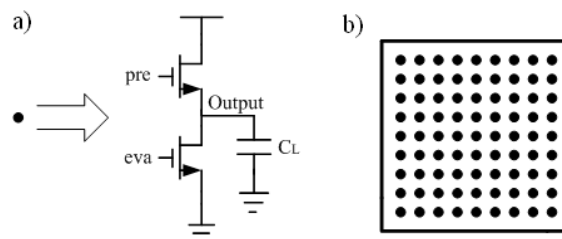


Fig.4 a) Random-variation sensor; b) Sensor set



measure; 2) it can also eliminate the effect of device parasitic capacitances and thus simplify the complexity of theoretical analysis, as shown in subsequent sections. As a result, deviations of fall and rise times in the output can be attributed to variations in *eva* and *pre* xnwFETs respectively. To determine the distribution of random variations in physical parameters, by statistical methods, a large number of such sensors are injected into the chip, defined as the sensor set (as shown in Fig. 4b).

Using this variation sensor, a variability sensing methodology is developed, which can estimate the distribution of random variations in physical parameters based on the measured fall and rise times of outputs in the sensor set. Table I summarizes the notations of parameters and variables used in the following sections.

	Notation	Distribution	
		Mean ( $\mu$ )	Standard Deviation ( $\sigma$ )
Rise Time	$t_r$	$\mu_{tr}$	$\sigma_{tr}$
Fall Time	$t_f$	$\mu_{ff}$	$\sigma_{ff}$
Channel Doping	$CD$	–	$\sigma_{CD}$
Source/drain Doping	$SDD$	–	$\sigma_{SDD}$
Underlap	$U$	–	$\sigma_U$
Complete Sensor Set	$n$	$\mu_c$	$\sigma_c$
Current Sensor Set	$m$	–	–
Log-likelihood Function	$L$	–	–
Estimation Error	$EE$	–	–
Average Estimation Error	$AEE$	–	–

### 3.1 MLE-based Variability Sensing Methodology

A general framework of Maximum Likelihood Estimation (MLE) based variability sensing methodology is shown in Fig. 5. A sensor set containing  $n$  distributed sensors can be used for variation sensing. We use MLE to calculate the mean and standard deviation of measured parameters. Variations in physical parameters will result in fluctuations of rise ( $t_r$ ) and fall ( $t_f$ ) times in each sensor. A set of  $t_r$  and  $t_f$  can be measured from the sensor set – marked as  $\{t_{r,1}, t_{r,2}, \dots, t_{r,n}\}$  and  $\{t_{f,1}, t_{f,2}, \dots, t_{f,n}\}$ . Assuming that  $t_r$  and  $t_f$  follow normal distributions ( $N(\mu_{tr}, \sigma_{tr})$ ,  $N(\mu_{ff}, \sigma_{ff})$ ) with unknown mean ( $\mu$ ) and unknown standard deviation ( $\sigma$ ), MLE can be employed to calculate their mean and standard deviation. Eq. (1) and (2) shows both mean ( $\mu$ ) and standard deviation ( $\sigma$ ) calculations, given the sample set  $\{t_{r,1}, t_{r,2}, \dots, t_{r,n}\}$  and  $\{t_{f,1}, t_{f,2}, \dots, t_{f,n}\}$ .

$$\mu_{ff/tr} = \frac{1}{n} \sum_{i=1}^n t_{f/r,i} \quad (1)$$

$$\sigma_{ff/tr}^2 = \frac{1}{n} \sum_{i=1}^n (t_{f/r,i} - \mu_{ff/tr})^2 \quad (2)$$

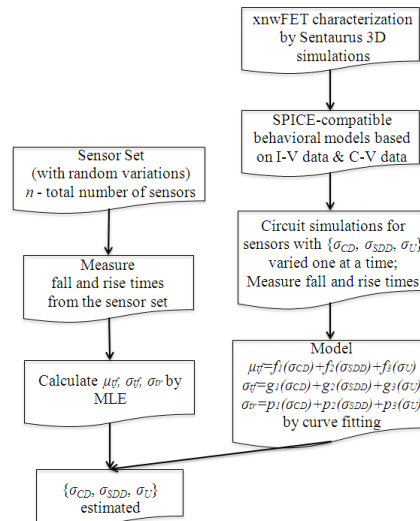


Fig.5 Maximum Likelihood Estimation (MLE) based variability sensing methodology

The fluctuations in rise and fall times in each sensor are directly correlated to the variations in *pre* and *eva* xnwFET transistors. We can assume mean and standard deviation of  $t_r$  and  $t_f$  as functions of standard deviations of random parameters, as expressed by the set of equations in (3).

$$\begin{cases} \mu_{t_f} = f(\sigma_{X_1}, \sigma_{X_2}, \dots, \sigma_{X_N}) \\ \sigma_{t_f} = g(\sigma_{X_1}, \sigma_{X_2}, \dots, \sigma_{X_N}) \\ \mu_{t_r} = h(\sigma_{X_1}, \sigma_{X_2}, \dots, \sigma_{X_N}) \\ \sigma_{t_r} = p(\sigma_{X_1}, \sigma_{X_2}, \dots, \sigma_{X_N}) \end{cases} \quad (3)$$

In (3),  $f(\sigma)$ ,  $g(\sigma)$ ,  $h(\sigma)$  and  $p(\sigma)$ , respectively, are shown as functions of standard deviations of physical parameters  $\{X_1, X_2, \dots, X_N\}$ .

Specifically, for random parameter variation estimation in the NASIC fabric we mainly focus on three physical parameters: channel doping (*CD*), source-drain doping (*SDD*) and underlap (*U*). To estimate the distributions of these random parameters, we use the equation set (4), based on (3).

$$\begin{cases} \mu_{t_f} = f(\sigma_{CD}, \sigma_{SDD}, \sigma_U) \\ \sigma_{t_f} = g(\sigma_{CD}, \sigma_{SDD}, \sigma_U) \\ \mu_{t_r} = h(\sigma_{CD}, \sigma_{SDD}, \sigma_U) \\ \sigma_{t_r} = p(\sigma_{CD}, \sigma_{SDD}, \sigma_U) \end{cases} \quad (4)$$

Since each of our parameters is mainly dependent on a separate process step, we assume that variations in these parameters are independent from each other. As a result, (4) can be decomposed into functions of the individual parameters, as shown in (5).

$$\begin{cases} \mu_{t_f} = f_1(\sigma_{CD}) + f_2(\sigma_{SDD}) + f_3(\sigma_U) \\ \sigma_{t_f} = g_1(\sigma_{CD}) + g_2(\sigma_{SDD}) + g_3(\sigma_U) \\ \mu_{t_r} = h_1(\sigma_{CD}) + h_2(\sigma_{SDD}) + h_3(\sigma_U) \\ \sigma_{t_r} = p_1(\sigma_{CD}) + p_2(\sigma_{SDD}) + p_3(\sigma_U) \end{cases} \quad (5)$$

To derive the functions in equation set (5), a device behavioral model encompassing parameter variations is built first. The xnwFET device structure is extensively characterized through variation-aware 3-D physics based simulations using Synopsys Sentaurus tools [14]. Device *I-V* and *C-V* characteristics were obtained for up to  $3\sigma = \pm 30\%$  variations in all parameters; a standard deviation of  $\sigma = \pm 10\%$  was conservatively treated as worst-case scenario such as in [14]. The device characterization data was then used to build SPICE-compatible behavior models using regression analysis. These behavioral models represent the xnwFET resistance and capacitance as a function of gate-source voltage, drain-source voltage and extent of variation in physical parameters.

Using this device model, the equation set shown in (5) is populated in an initial circuit simulation step. Circuit simulations are carried out for the sensor shown in Fig. 4a – in this, standard deviations of random parameters are varied one at a time. Then, the relationship between  $\{\mu_{t_f}, \sigma_{t_f}, \mu_{t_r}, \sigma_{t_r}\}$  and  $\{\sigma_{CD}, \sigma_{SDD}, \sigma_U\}$  is built from the measured fall and rise times by curve fitting. Based on the circuit simulation results,  $\mu_{t_r}$  is almost constant with only 0.14% deviation as  $\{\sigma_{CD}, \sigma_{SDD}, \sigma_U\}$  increasing from 0 to 15%, which means  $\mu_{t_r}$  is irrelevant. Finally, the equation set is reduced as shown in (6) with known polynomial functions  $\{f_1, f_2, f_3, g_1, g_2, g_3, p_1, p_2, p_3\}$  from curve fitting.

$$\begin{cases} \mu_{t_f} = f_1(\sigma_{CD}) + f_2(\sigma_{SDD}) + f_3(\sigma_U) \\ \sigma_{t_f} = g_1(\sigma_{CD}) + g_2(\sigma_{SDD}) + g_3(\sigma_U) \\ \sigma_{t_r} = p_1(\sigma_{CD}) + p_2(\sigma_{SDD}) + p_3(\sigma_U) \end{cases} \quad (6)$$

Combining with the calculated  $\{\mu_{t_f}, \sigma_{t_f}, \sigma_{t_r}\}$  from MLE, standard deviations of random parameters are estimated by solving these equations as shown in Fig. 5.

There are two factors that can affect estimation accuracy: the precision of deriving equation set (6) and the accuracy of calculated  $\{\mu_{t_f}, \sigma_{t_f}, \sigma_{t_r}\}$ . Since (6) is derived by curve fitting in an initial circuit simulation step, it can be made increasingly more accurate by choosing more data points (i.e.,  $\{\sigma_{CD}, \sigma_{SDD}, \sigma_U\}$  and their corresponding  $\{\mu_{t_f}, \sigma_{t_f}, \sigma_{t_r}\}$ ) in the simulations. But the accuracy of calculated  $\{\mu_{t_f}, \sigma_{t_f}, \sigma_{t_r}\}$  depends on the size of sample set, corresponding to the size of the sensor set. In order to reduce the area overhead introduced by on-chip sensors, the sensor set is usually made as small as possible. As a result, the accuracy of the calculated  $\{\mu_{t_f}, \sigma_{t_f}, \sigma_{t_r}\}$  is constrained in practice, which may contribute to a large part of the estimation error. In the next section, we show how the mean and standard deviation calculations can be improved with reduced sample sets using the Expectation Maximization (EM) technique [25].

### 3.2 EM-based Variability Sensing Methodology

The Expectation Maximization (EM) algorithm [25] is an efficient alternative to MLE in the calculation of  $\{\mu_{t_f}, \sigma_{t_f}, \sigma_{t_r}\}$ . It is an iterative method for estimating the values of some unknown parameters in a statistical model. It can enable more accurate

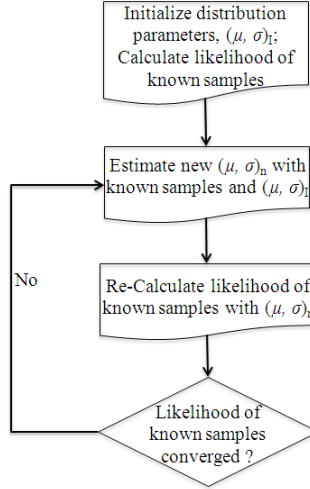


Fig.6 Flowchart of Expectation Maximization algorithm

parameter estimation in a statistical model even with incomplete sample set. It is made possible by filling the missing samples with the expected value of the complete samples and iterating sufficient times until the likelihood of known samples is maximized. In this algorithm, there are two sample sets: the complete sample set (i.e., an imaginary sample set that contains sufficient samples to achieve converged estimates) and the current sample set employed. The number of missing samples equals to the difference in the sizes of these two sample sets. A general framework of EM algorithm for normal distribution is shown in Fig. 6.

Based on Fig. 6, the EM algorithm is iterated enough times until the convergence of the likelihood is reached, treated as the maximum of this likelihood. In this algorithm, the initial values of  $(\mu, \sigma)$  affect the estimation accuracy and overall run-time, and should be therefore chosen carefully.

In our case, if the size of the complete sensor set is  $n$  and the size of current sensor set employed is  $m$ , the number of missing sensors equals  $n-m$ . Let  $\{t_{r,1}, t_{r,2}, \dots, t_{r,m}\}$  and  $\{t_{f,1}, t_{f,2}, \dots, t_{f,m}\}$  denote the measured rise and fall times from the current sensor set, and  $\{t_{r,m+1}, t_{r,m+2}, \dots, t_{r,n}\}$ , as well as  $\{t_{f,m+1}, t_{f,m+2}, \dots, t_{f,n}\}$ , denote the unknown measurements from the missing sensors. As the part of the process of EM in the calculation of the mean and standard deviation of  $t_r$  and  $t_f$  is completed in a similar manner, we only use fall times ( $t_f$ ) to illustrate how EM algorithm calculates the mean and standard deviation from an incomplete sensor set. This is as follows.

- 1 Estimate an initial  $(\mu, \sigma)_C$  for the complete sensor set,  $\{t_{f,1}, t_{f,2}, \dots, t_{f,m}, t_{f,m+1}, t_{f,m+2}, \dots, t_{f,n}\}$ ;
- 2 Calculate the log-likelihood function, given known  $\{t_{f,1}, t_{f,2}, \dots, t_{f,m}\}$  under this initial  $(\mu, \sigma)_C$  by Eq. (7);

$$L(t_f) = -0.5n * \log(2\pi * \sigma_C^2) - 0.5 \sum_{i=1}^m (t_{f,i} - \mu_C)^2 / \sigma_C^2 \quad (7)$$

- 3 Re-estimate  $(\mu, \sigma)_C$  by Eq. (8) and (9);

$$\mu_{C,i} = \frac{1}{n} \sum_{i=1}^m t_{f,i} + \frac{n-m}{n} \mu_{C,i-1} \quad (8)$$

$$\sigma_{C,i}^2 = \frac{1}{n} \left[ \sum_{i=1}^m t_{f,i}^2 + (n-m) * (\mu_{C,i-1}^2 + \sigma_{C,i-1}^2) \right] - \mu_{C,i}^2 \quad (9)$$

- 4 Re-calculate the log-likelihood function given known  $\{t_{f,1}, t_{f,2}, \dots, t_{f,m}\}$  under the new  $(\mu, \sigma)_C$  by Eq. (7);
- 5 Repeat until the convergence of the log-likelihood function.

The condition of convergence is expressed as Eq. (10),

$$\left| L(t_f)_{new} - L(t_f)_{old} \right| < \varepsilon \quad (10)$$

where  $\varepsilon$  is very small and depends on the required accuracy.

Fig. 7 shows our random variation sensing methodology, which uses EM algorithm for mean and standard deviation calculation. Compared with the previous MLE-based estimation methodology, the main difference is that in the estimation flow we replaced MLE (for the calculation of mean and standard deviation of fall and rise times) by the EM algorithm.

#### 4. Evaluation of the Proposed Sensor Design

In this section we detail a framework for evaluating the accuracy of our sensor design based on Monte Carlo circuit simulations. The framework is shown in Fig. 8.

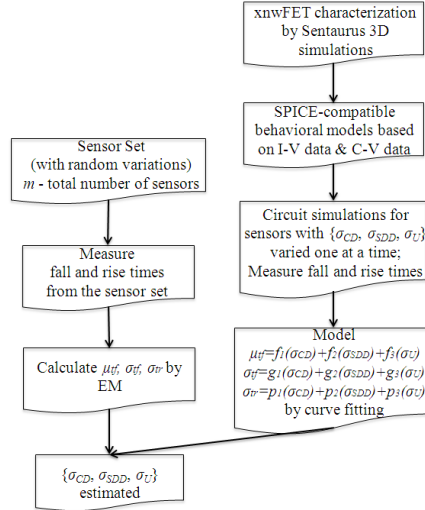


Fig.7 Expectation Maximization (EM) based variability sensing methodology

As shown in Fig. 8a, HSPICE circuit simulations need to be carried out with known variation cases injected into the sensor circuits. These simulations assume normal distributions of individual device parameters with a known standard deviation. Based on the measured fall and rise times from the sensor circuits, the standard deviation of random parameters is estimated using the theoretical framework described in the previous sections. As statistical methods are used in the proposed methodology, the number of samples becomes very important to the estimation accuracy. The number of sensors in the sensor set is varied to demonstrate how it affects the estimation accuracy. HSPICE circuit simulations on the sensor set are iterated 1,000 times to achieve sufficient estimates for  $\{\sigma_{CD}, \sigma_{SDD}, \sigma_U\}$ . The probability density functions (PDF) of these estimated standard deviations are built to check the degree of convergence. Then the relative errors in estimated vs. injected standard deviations of random parameters are calculated. This iterative flow is abstracted in Fig. 8b.

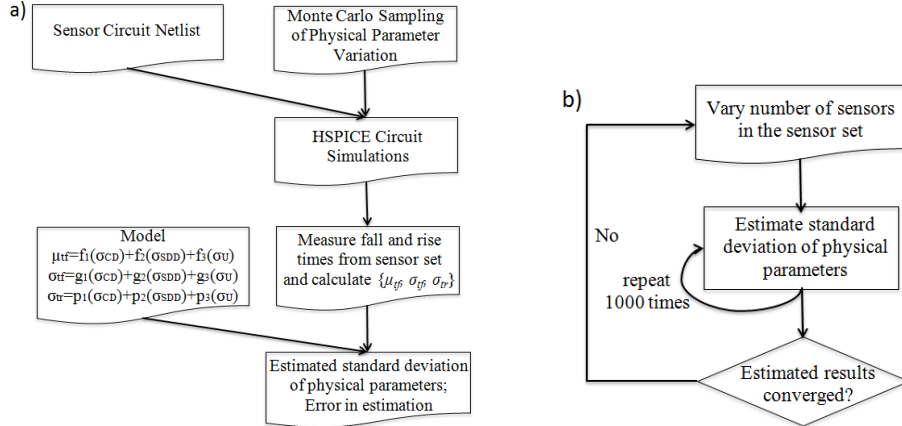


Fig.8 Framework for evaluating sensor design based on Monte Carlo circuit simulations: a) Evaluation flow; b) Details on Monte Carlo circuit simulations

## 5. Results

Following the evaluation framework described in the previous section, circuit simulations were carried out to determine the accuracy of the sensing method for random variation estimation. In the equation set (6), based on the accuracy of curve fitting,  $f(\sigma)$  was populated as a fifth-order polynomial;  $g(\sigma)$  and  $p(\sigma)$  were populated as third-order polynomials. The simulations were iterated for 1,000 times to estimate  $\{\sigma_{CD}, \sigma_{SDD}, \sigma_U\}$  sets. The metrics used are Estimation Error ( $EE$ ) and Average Estimation Error ( $AEE$ ) for parameter  $X_i$  across 1,000 estimated results. We defined these as:

$$EE = \left| \frac{\sigma_{X_i}^e - \sigma_{X_i}^i}{\sigma_{X_i}^i} \right| \quad (11)$$

$$AEE = (EE^1 + EE^2 + \dots + EE^{1000}) / 1000 \quad (12)$$

wherein  $\sigma_{X_i}^e$  is the estimated standard deviation of parameter  $X_i$ , and  $\sigma_{X_i}^i$  is the injected standard deviation of parameter  $X_i$  in the simulations;  $EE^j$  represents the  $j$ th estimation error of one parameter across 1,000 iterations.

### 5.1 Simulation Results of MLE-based Sensing Method

Fig. 9 shows the probability density function (PDF) of estimated standard deviations for varying number of sensors in the sensor set. The estimated standard deviations gradually converge and approach the injected value (0.1) as the number of sensors in the sensor set ( $n$ ) increases. For example, when  $n$  increases from 50 to 200,  $\sigma$  in PDF of estimated  $\sigma_U$  decreases from 0.022 to 0.007, which means the degree of convergence in  $\sigma_U$  is increased by 3X. However, when  $n$  increases from 200 to 250, the improvement in the convergence of estimated  $\{\sigma_{CD}, \sigma_{SDD}, \sigma_U\}$  becomes less significant; a less than 10% decrease in  $\sigma$  of PDFs of the estimated  $\{\sigma_{CD}, \sigma_{SDD}, \sigma_U\}$  is in fact achieved. This means that 200 sensors in the sensor set are sufficient to estimate  $\{\sigma_{CD}, \sigma_{SDD}, \sigma_U\}$  such that they are less than or equal to 0.1.

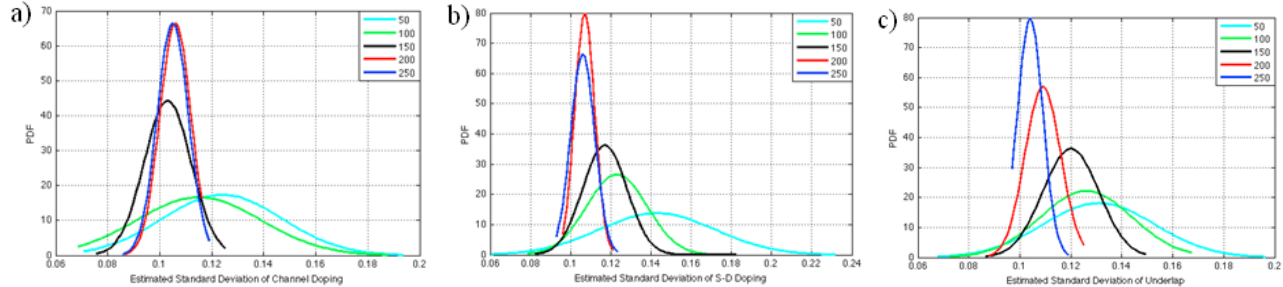


Fig.9 Probability density function (PDF) of estimated standard deviation for varying number of sensors in the sensor set; a) Channel doping; b) Source-Drain doping; and c) Underlap

For the sensor set containing 200 sensors, the estimation error for every parameter was calculated. The corresponding cumulative distribution function (CDF) of estimation error across 1,000 estimated results is shown in Fig. 10. From this figure, we can note that the estimation error is largest for the underlap variation; however, this error is still less than 15% for 90% of simulations and smaller than 25% for all simulated cases. Estimation errors of all three parameters for worst-case scenarios are summarized in Table II.

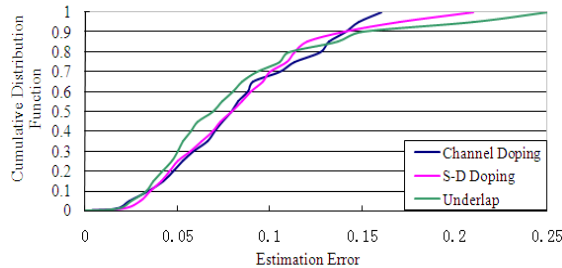


Fig.10 Cumulative distribution function (CDF) of estimation error across 1,000 estimated standard deviations

TABLE II. ESTIMATION ERROR FOR MLE-BASED SENSING METHOD			
	Underlap	Channel doping	SD doping
<i>EE</i> in worst-case scenario	25% (most sensitive)	16% (least sensitive)	20%

## 5.2 Simulation Results of EM-based Sensing Method

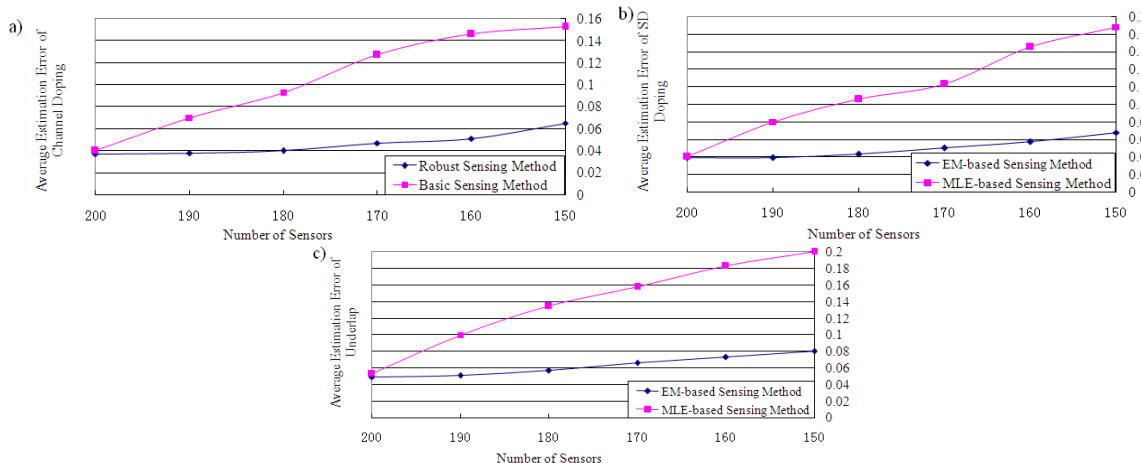


Fig.11 Comparison of average estimation error (AEE) between EM-based and MLE-based sensing methods: a) Channel doping; b) Source-Drain doping; c) Underlap.

For EM-based sensing method, the size of complete sensor set ( $n$ ) was set to 200 and was kept constant for simulations. Fig. 11 shows the comparison of  $AEE$  for MLE-based and EM-based sensing methods.  $AEE$  is much smaller for the EM-based sensing method than the MLE-based sensing method. For example, for underlap ( $U$ ), if the number of sensors in the current sensor set ( $m$ ) decreases from 200 to 150,  $AEE$  increases from 0.053 to 0.2 with the MLE-based sensing method, but only increases from 0.049 to 0.08 with the EM-based sensing method. As a result, the estimated results become more robust with decrease in number of sensors and the estimation accuracy is improved by at least 2X with the EM-based sensing method. The results are presented in Table III, which shows a range of  $AEEs$  due to varying number of sensors from 200 to 150.

TABLE III. COMPARISON OF  $AEE$  BETWEEN EM-BASED METHOD AND MLE-BASED METHOD

	$m$ decreased from 200 to 150		
	$AEE$ of $CD$	$AEE$ of $SDD$	$AEE$ of $U$
EM-based method	[0.037,0.065]	[0.039,0.068]	[0.049,0.08]
MLE-based method	[0.04,0.153]	[0.04,0.188]	[0.053,0.2]

For the EM-based sensing method, the number of sensors in the sensor set was gradually decreased to evaluate how estimation accuracy is impacted. The relationship between  $AEE$  and the number of sensors in the sensor set is shown in Fig. 12. The estimated standard deviation of underlap has the largest  $AEE$  among the three random parameters. If  $AEE$  is required to be less than 10%, at least 150 sensors are needed in the sensor set.

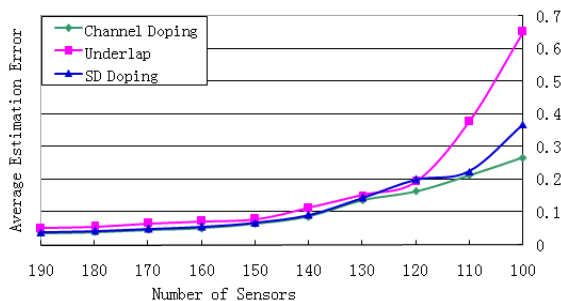


Fig.12 Relationship between average estimation error and number of sensors

For  $m=150$ , the cumulative distribution function of the estimation error is shown in Fig. 13. From these results,  $EE$  is largest for the underlap variation with 12.7% (for all simulations), which can be treated as worst-case scenario.  $EEs$  in the worst-case scenario for all three parameters are listed in Table IV. Compared with the  $EEs$  in Table II, the estimation accuracy is improved by 2X with the EM-based sensing method.

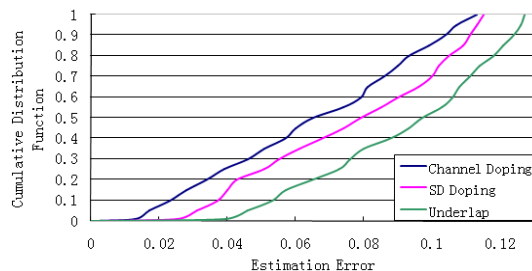


Fig.13 Cumulative distribution function of estimation error for  $m=150$  current sensor set

TABLE IV. ESTIMATION ERROR FOR EM-BASED SENSING METHOD

	Underlap	Channel doping	SD doping
$EE$ in worst-case scenario	12.7% (most sensitive)	11.3% (least sensitive)	11.5%

In order to evaluate the proposed EM-based sensing method more extensively, the injected standard deviation of physical parameters was reduced gradually from 10% to 1% in the Monte Carlo simulations; we then re-estimated the error with the EM-based sensing method. Following the evaluation flow shown in Fig. 8, the worst-case estimation errors were calculated. Fig. 14 shows the relationship between worst-case estimation errors and injected standard deviations of physical parameters. For these simulations number of sensors in the sensor set was fixed to 150. From these results, the worst-case estimation error decreases slightly (as the injected standard deviation of physical parameters). The main reason for this slight decrease in the

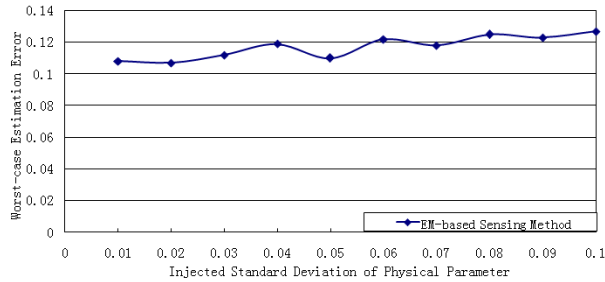


Fig.14 Relationship between the worst-case estimation error and the injected standard deviation of physical parameter for m=150

worst-case estimation error is the increase of the accuracy in the calculation of  $\{\mu_{tf}, \sigma_{tf}, \sigma_{tr}\}$ . As the standard deviation of a physical parameter decreases, the degree of fluctuation in the fall and rise times also decreases, which means the number of samples required to derive the distribution decreases. However, the number of sensors in all simulations remains constant, so the accuracy of calculated  $\{\mu_{tf}, \sigma_{tf}, \sigma_{tr}\}$  improves. From Fig. 14, the worst-case estimation error is less than 13% with the EM-based sensing method for all standard deviations that are less than or equal to 10%.

## 6. Conclusion

A new on-chip variation sensor design for random variation estimation in the NASIC fabric was presented. A generic sensing methodology for extracting distributions of random variations in physical parameters from the measured fall and rise times was described. Using physics-based device models and Monte Carlo simulations, sensing estimation accuracy was quantified. Simulation results show that with the EM-based variability sensing estimation method, an 8% average estimation error can be achieved with as low as 150 sensors in the sensor set. The estimation error in the worst-case scenario was 12.7% for all simulated cases. This result indicates the feasibility of the outlined approach. Furthermore, we believe that the proposed on-chip variation sensors when applied in conjunction with post-fabrication compensation techniques would be able to improve system-level performance in nanoscale computing fabrics; this is an efficient alternative to making worst-case assumptions on parameter variations in nanoscale designs.

## References

- [1] T. Wang, M. Bennaser, Y. Guo, C. A. Moritz, "Wire-Streaming Processors on 2-D Nanowire Fabrics," NSTI (Nano Science and Technology Institute) Nanotech 2005, California, May 2005.
- [2] T. Wang, M. Bennaser, Y. Guo, C. A. Moritz, "Self-Healing Wire-Streaming Processors on 2-D Semiconductor Nanowire Fabrics," NSTI (Nano Science and Technology Institute) Nanotech 2006, Boston, MA, May 2006.
- [3] S. Iijima and T. Ichihashi, "Single-shell carbon nanotubes of 1-nm diameter," *Nature*, vol. 363, no. 6430, pp. 603–605, June 1993.
- [4] S. Khasanvis, et al., "Hybrid Graphene Nanoribbon-CMOS Tunneling Volatile Memory Fabric," *IEEE/ACM International Symposium on Nanoscale Architectures (NANOARCH)*, pp.189-195, 8-9 June 2011.
- [5] S. Khasanvis, et al., "Ternary Volatile Random Access Memory based on Heterogeneous Graphene-CMOS Fabric," to appear in *Proceedings of IEEE/ACM International Symposium on Nanoscale Architectures (NanoArch)*, 2012.
- [6] P. Shabadi, A. Khitun, K. Wong, P. Khalili Amiri, K. L. Wang and C. A. Moritz, "Spin Wave Functions Nanofabric Update," *IEEE/ACM International Symposium on Nanoscale Architectures (NANOARCH)*, pp.107-113, 8-9 June 2011.
- [7] P. Shabadi and C. A. Moritz, "Post-CMOS Hybrid Spin-Charge Nanofabrics," *IEEE International Conference on Nanotechnology (IEEE NANO 2011)*, pp.1399-1402, 15-18 Aug. 2011.
- [8] P. Shabadi, S. Rajapandian, S. Khasanvis, and C. A. Moritz, "Design Of Spin Wave Functions-Based Logic Circuits," in *SPIN*, vol. 2, no. 3, 2012.
- [9] D. J. Palframan, N. S. Kim, and M. H. Lipasti, "Mitigating Random Variation with Spare RIBs: Redundant Intermediate Bitslices," *IEEE/IFIP international conference on Dependable Systems and Networks (DSN)*, 2012.
- [10] R. Teodorescu et al., "Mitigating parameter variation with dynamic fine-grain body biasing," in *Proc. MICRO-40*, Chicago, IL, Dec. 2007, pp. 27–39.
- [11] B. Wan, J. Wang, G. Keskin, and L. T. Pileggi, "Ring Oscillators for Single Process-Parameter Monitoring," in *Proc. Workshop on Test Structure Design for Variability Characterization*, 2008.
- [12] I. A. K. M. Mahfuzul, A. Tsuchiya, K. Kobayashi, and H. Onodera, "Process-sensitive Monitor Circuits for Estimation of Die-to-Die Process Variability," in *Proc. TAU*, 2010, pp. 83–88.
- [13] D. Blaauw, K. Chopra, A. Srivastava, and L. Scheffer, "Statistical Timing Analysis: From Basic Principles to State of the Art," *IEEE Transactions on CAD*, vol. 27, no. 4, pp. 589–607, 2008.
- [14] P. Narayanan, M. Leuchtenburg, J. Kina, P. Joshi, P. Panchapakeshan, C. O. Chui and C. A. Moritz, "Parameter Variability in Nanoscale Fabrics: Bottom-Up Integrated Exploration," *IEEE 25th International Symposium on Defect and Fault Tolerance in VLSI Systems (DFT)*, pp.24-31, 2010.
- [15] C. A. Moritz, P. Narayanan, and C. O. Chui, "Nanoscale application specific integrated circuits," N. K. Jha and D. Chen, Eds. Springer New York, pp. 215–275, 2011.
- [16] P. Narayanan, et al., "Nanoscale Application Specific Integrated Circuits," *IEEE/ACM International Symposium on Nanoscale Architectures (NANOARCH)*, pp.99-106, 2011.
- [17] P. Narayanan, et al., "CMOS Control Enabled Single-Type FET NASIC," in *IEEE Computer Society Annual Symposium on VLSI*, pp.191-196, 2008.
- [18] T. Wang, P. Narayanan, M. Leuchtenburg, C. A. Moritz, "NASICs: A Nanoscale Fabric for Nanoscale Microprocessors," *IEEE International Nanoelectronics Conference (INEC)*, 2008.
- [19] C. A. Moritz, et al., "Fault-Tolerant Nanoscale Processors on Semiconductor Nanowire Grids," *IEEE Transactions on Circuits and Systems I*, special issue on Nanoelectronic Circuits and Nanoarchitectures, vol. 54, iss. 11, pp. 2422-2437, November 2007.
- [20] P. Panchapakeshan, P. Narayanan and C. A. Moritz, "N3ASIC: Designing Nanofabrics with Fine-Grained CMOS Integration," *IEEE/ACM International Symposium on Nanoscale Architectures (NANOARCH)*, pp.196-202, 8-9 June 2011.

- [21] M. Rahman, P. Narayanan and C. A. Moritz, "N3ASIC Based Nanowire Volatile RAM," IEEE International Conference on Nanotechnology (IEEE NANO 2011), pp.1097-1101, 15-18 Aug. 2011.
- [22] M. Collins, B. M. Al-Hashimi and N. Ross, "A Programmable Time Measurement Architecture for Embedded Memory Characterization," Test Symposium, 2005 European, pp. 128-133, 2005.
- [23] K. Shinkai and M. Hashimoto, "Device-Parameter Estimation with On-Chip Variation Sensors Considering Random Variability," Proc. ASP-DAC, pp. 683-688, 2011.
- [24] J. Zhang, et al., "On-Chip Variation Sensor for Systematic Variation Estimation in Nanoscale Fabrics," IEEE International Conference on Nanotechnology (IEEE NANO 2012), 20-23 Aug. 2012.
- [25] A. Dempster, N. Laird, and D. Rubin, "Maximum Likelihood From Incomplete Data Via the EM Algorithm," Journal of the Royal Statistical Society, Series B, vol. 39(1), pp. 1-38, 1977.



## Figure Caption

- Fig.1 Nanoscale Application Specific Integrated Circuits with regular semiconductor nanowire grids, xnwFET devices and peripheral microscale control a) 3-D fabric view b) circuit schematic
- Fig.2 *N-input* NASIC dynamic NAND gate
- Fig.3 n-type xnwFET device structure with orthogonal gate and channel nanowires
- Fig.4 a) Random-variation sensor; b) Sensor set
- Fig.5 Maximum Likelihood Estimation (MLE) based variability sensing methodology
- Fig.6 Flowchart of Expectation Maximization algorithm
- Fig.7 Expectation Maximization (EM) based variability sensing methodology
- Fig.8 Framework for evaluating sensor design based on Monte Carlo circuit simulations: a) Evaluation flow; b) Details on Monte Carlo circuit simulations
- Fig.9 Probability density function (PDF) of estimated standard deviation for varying number of sensors in the sensor set; a) Channel doping; b) Source-Drain doping; and c) Underlap
- Fig.10 Cumulative distribution function (CDF) of estimation error across 1,000 estimated standard deviations
- Fig.11 Comparison of average estimation error (*AEE*) between EM-based and MLE-based sensing methods: a) Channel doping; b) Source-Drain doping; c) Underlap
- Fig.12 Relationship between average estimation error and number of sensors
- Fig.13 Cumulative distribution function of estimation error for  $m=150$  current sensor set
- Fig.14 Relationship between the worst-case estimation error and the injected standard deviation of physical parameter for  $m=150$

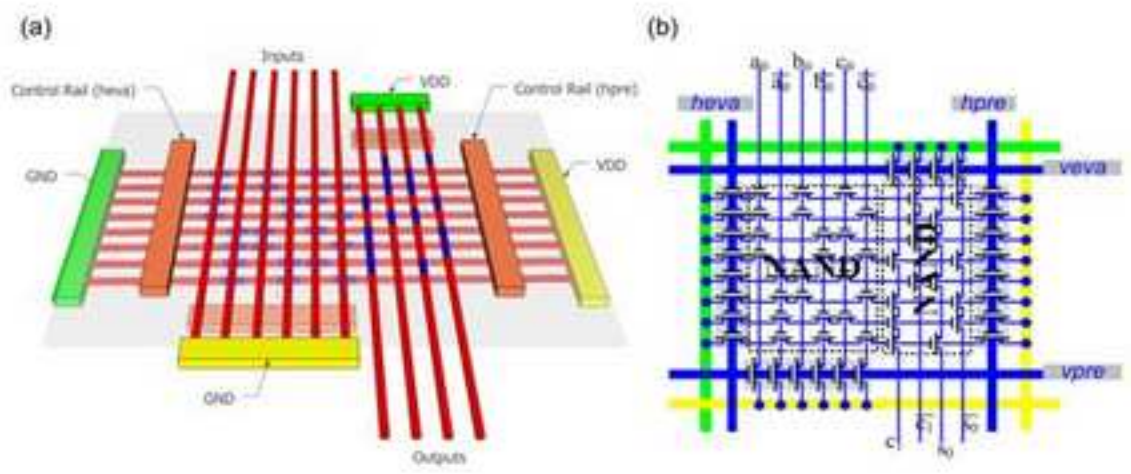


FIG2.JPEG

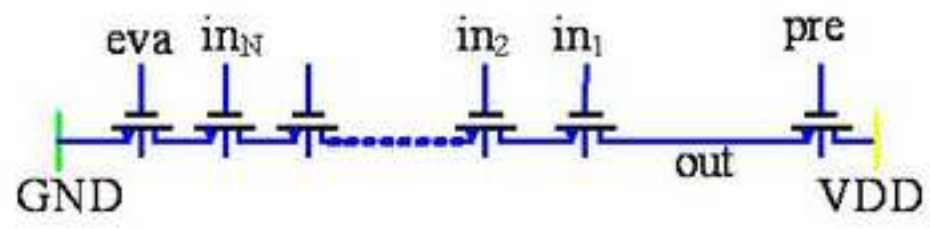
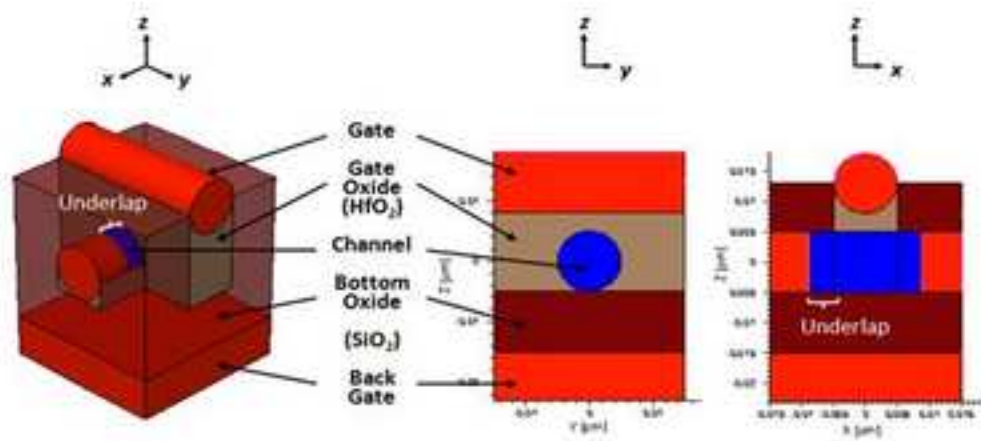
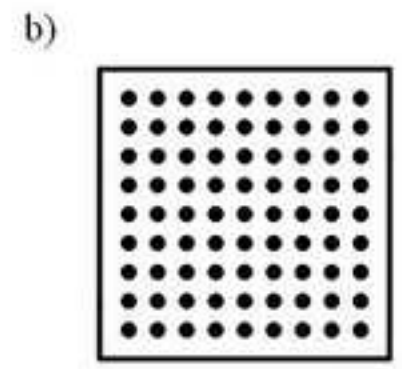
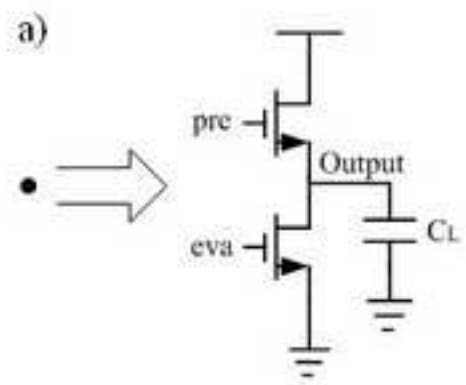
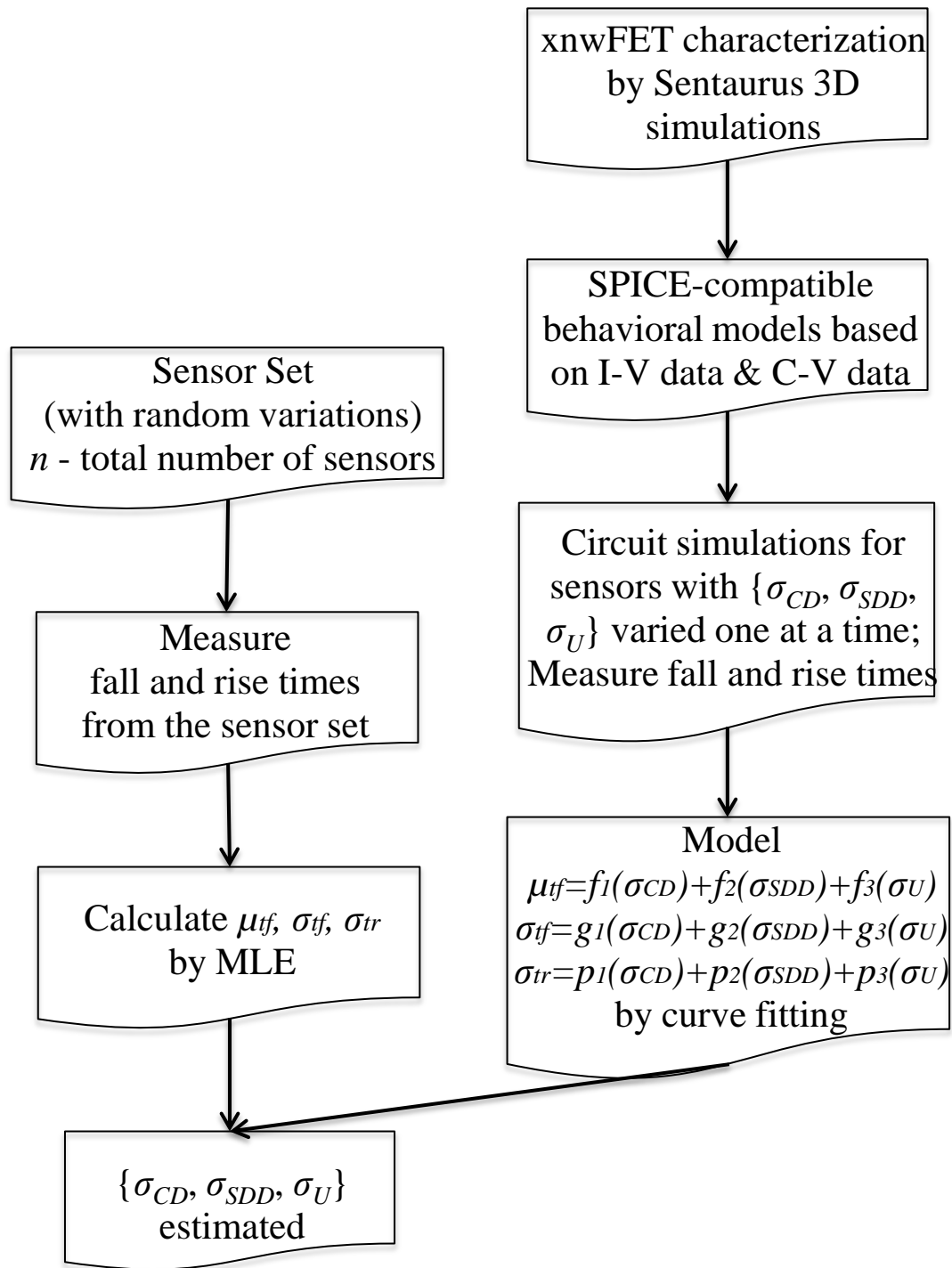
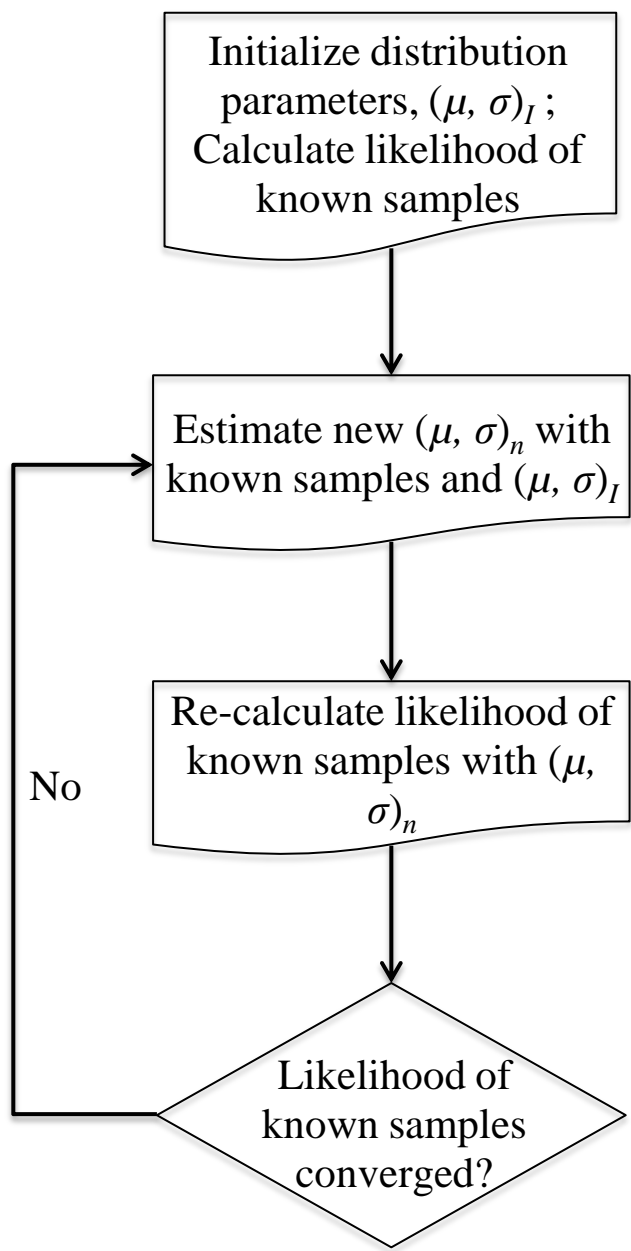


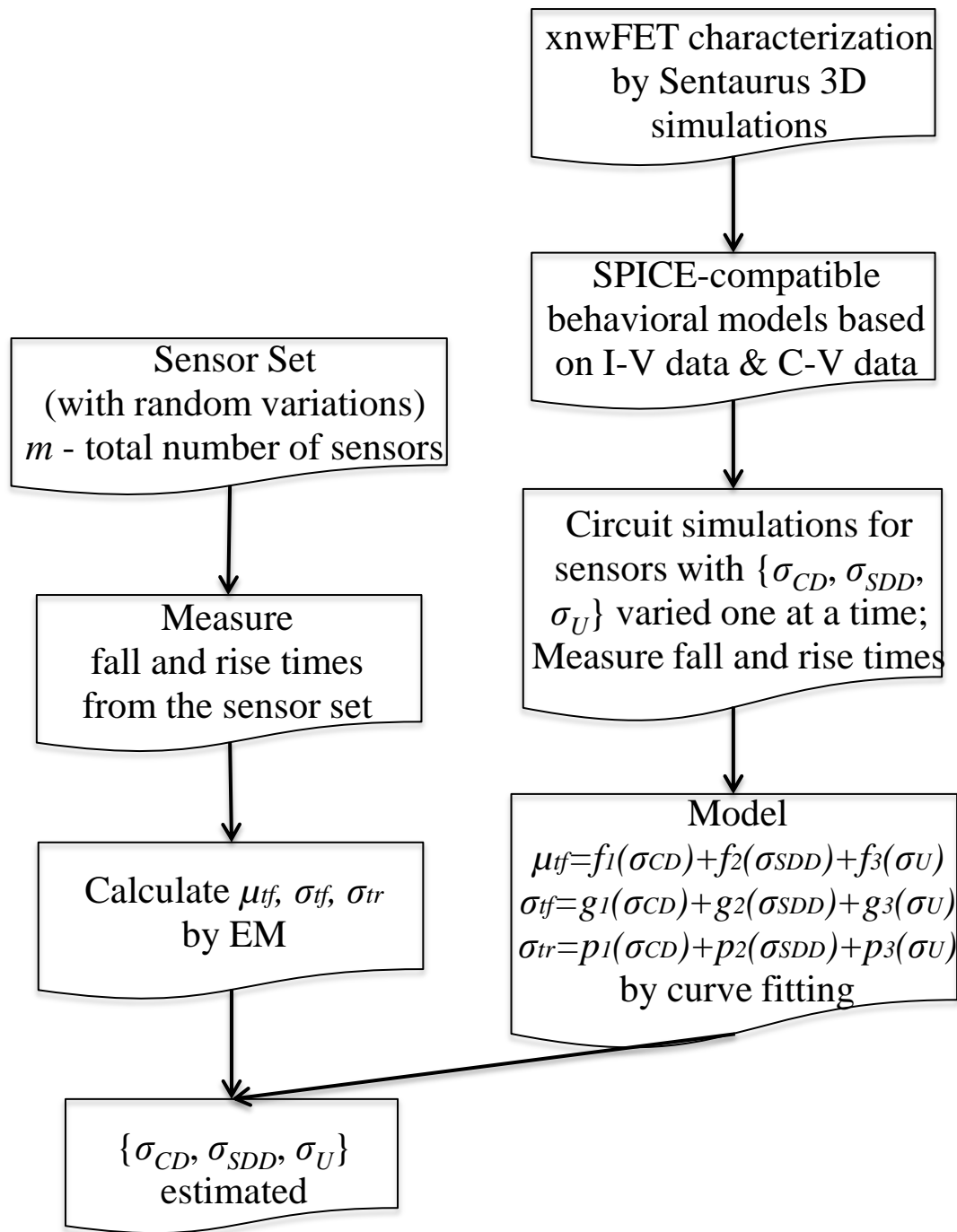
FIG3.JPEG





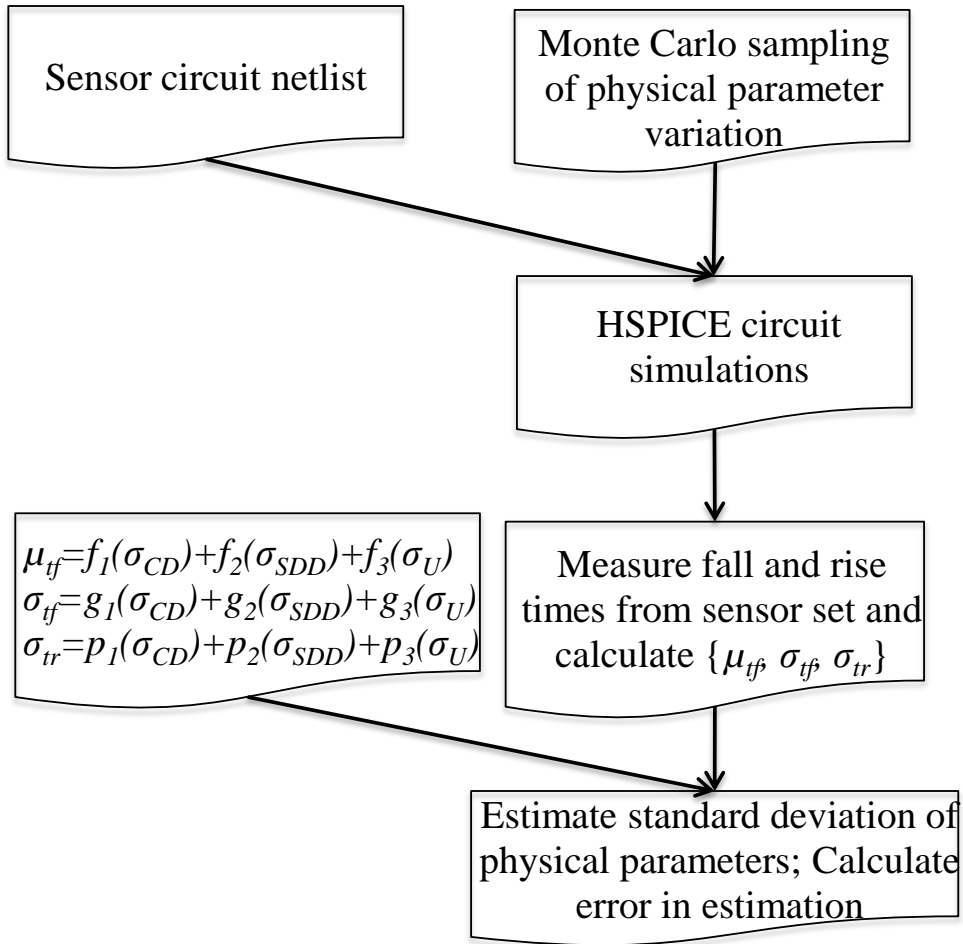








a)



b)

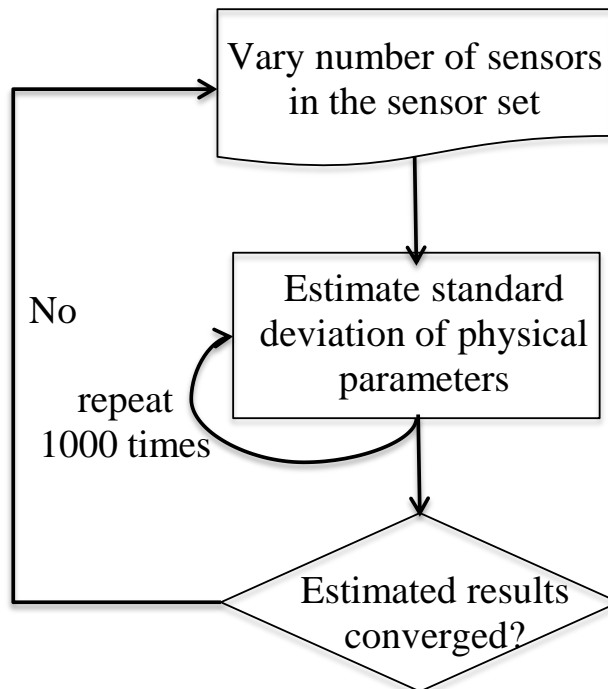


FIG9.JPEG

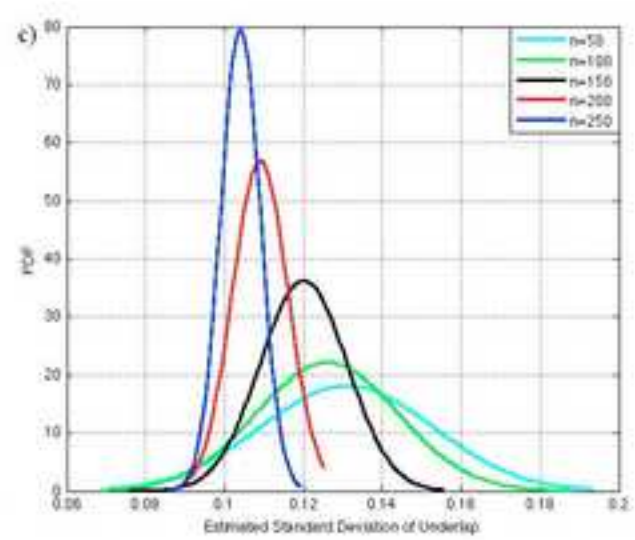
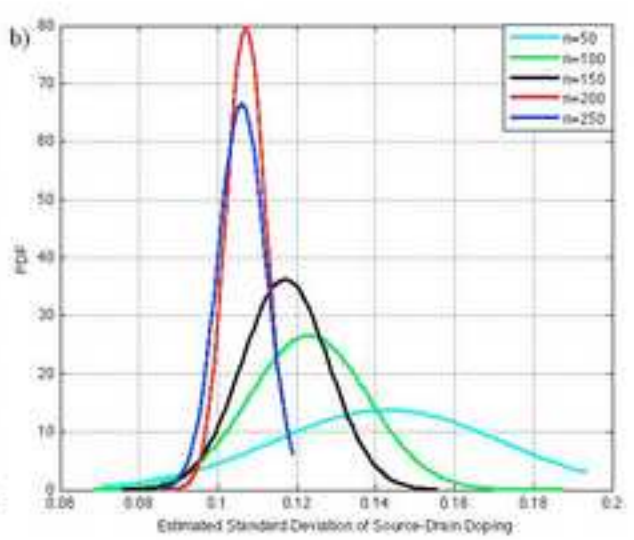
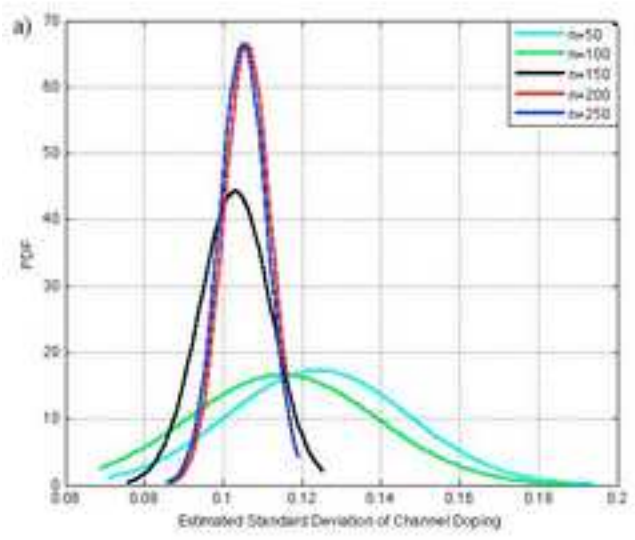
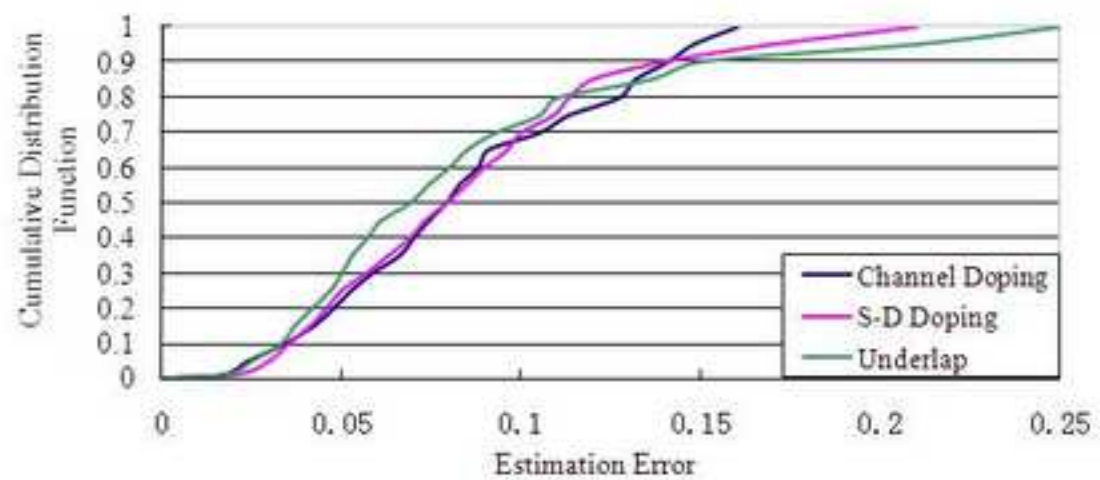
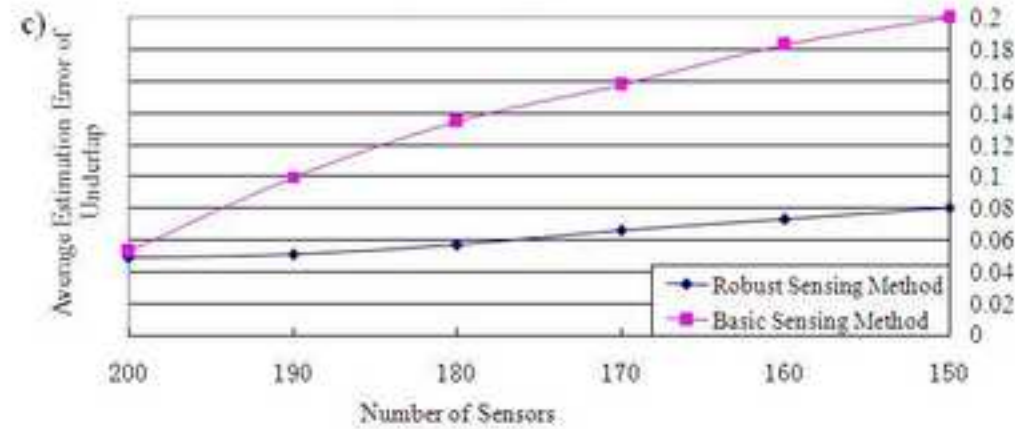
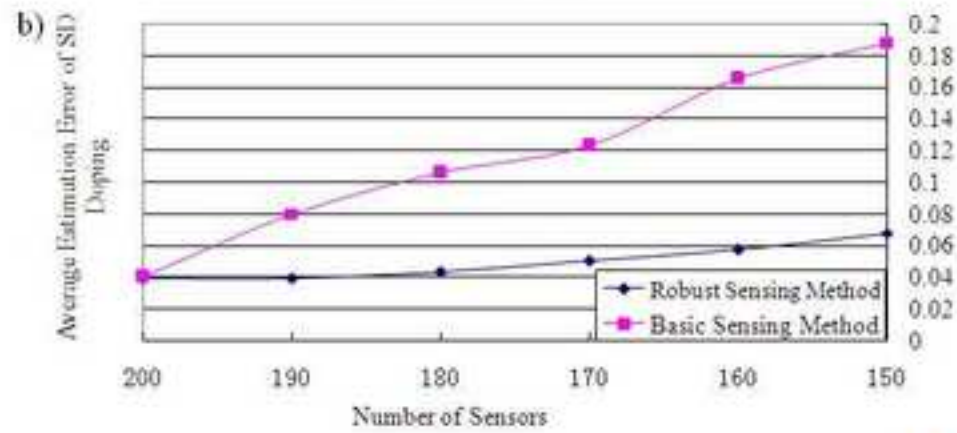
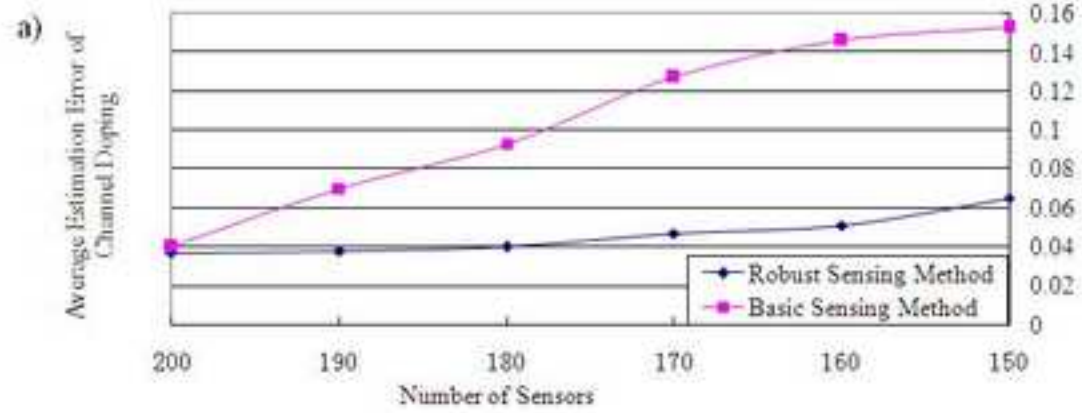
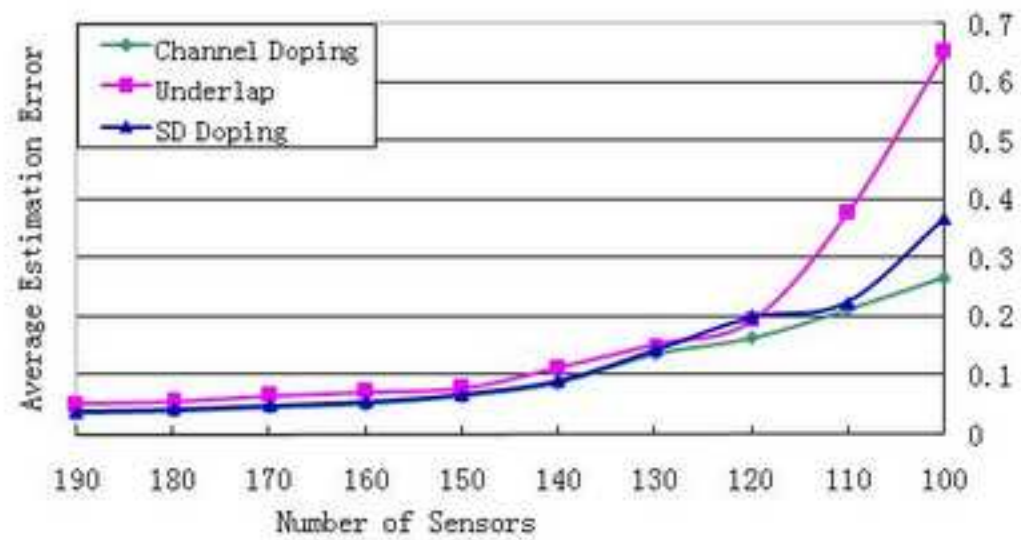
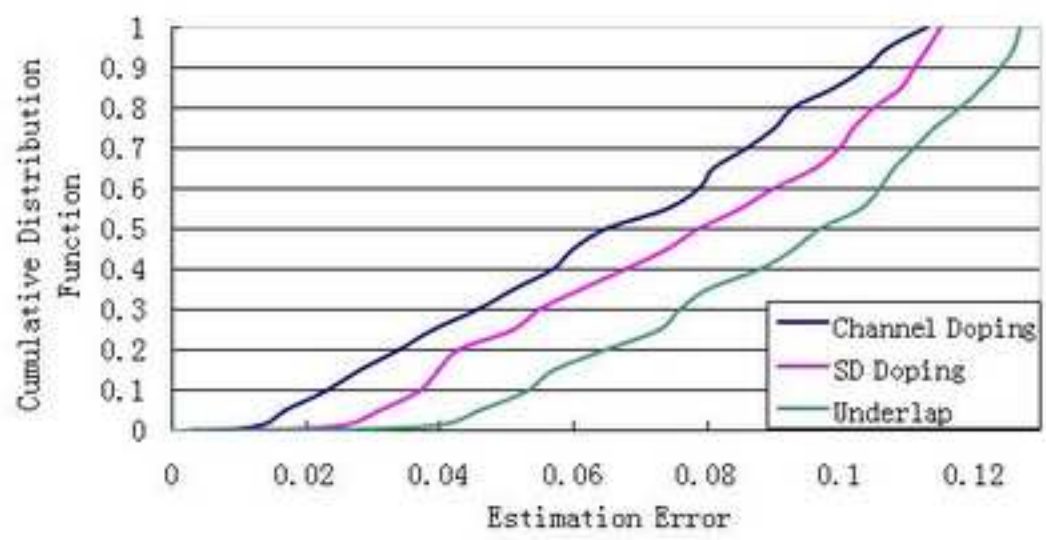


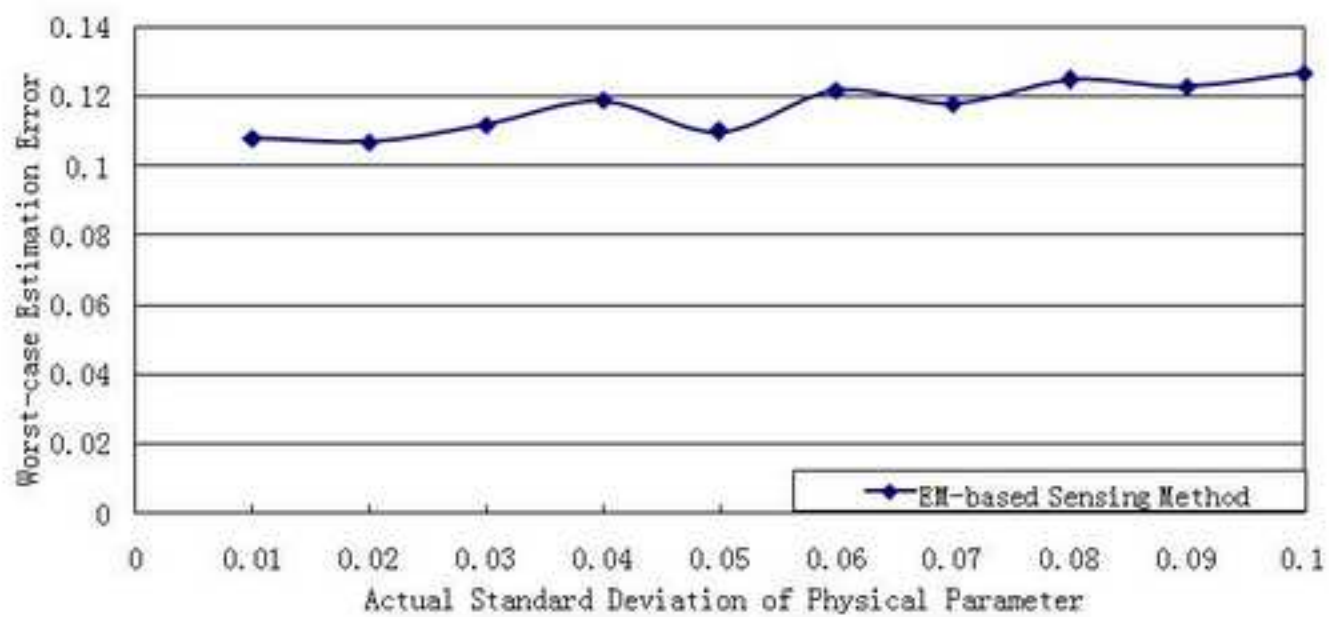
FIG10.JPEG












	<p><b>Jianfeng Zhang</b> received the B.E. degree in electrical and computer engineering from the Harbin Institute of Technology, Harbin, China, in 2010. He is currently working toward the M.S. degree in electrical and computer engineering from the University of Massachusetts, Amherst.</p> <p>His research interests include nanoscale systems, computer architecture and VLSI design.</p>
	<p><b>Mostafizur Rahman</b> is currently a PhD student in Computer Engineering at University of Massachusetts Amherst. He works as a research assistant in nanoscale computing fabrics lab in Umass. His research has appeared in peer-reviewed conferences including IEEE Nanotechnology conference 2011, IEEE NanoArch 2011. He is also a reviewer for IEEE transactions on Nanotechnology journal. He received his Bachelor of Computer Engineering from North South University, Bangladesh in 2008.</p> <p>His research interests include post-CMOS computing techniques, emerging volatile and non-volatile memories, 3-D integration, semiconductor device physics, modeling, and simulation, nanoscale fabrication and characterization.</p>
	<p><b>Pritish Narayanan</b> received the B.E. (honors) degree in electrical and electronics engineering and the M.Sc. (honors) degree in chemistry from the Birla Institute of Technology and Science, Pilani, India, in 2005 and the Ph.D. degree in electrical and computer engineering from the University of Massachusetts, Amherst in 2013.</p> <p>At present he is a Research Staff Member at IBM Almaden Research Center. His research interests include nanoscale CMOS and post-CMOS logic and memory technologies, nano-fabrication and VLSI.</p> <p>Dr. Narayanan was a recipient of the Best Paper Award at ISVLSI 2008 and Best Student Paper Awards at IEEE DFT 2010 and 2011. He has served as a reviewer for IEEE TRANSACTIONS ON VLSI SYSTEMS, IEEE TRANSACTIONS ON NANOTECHNOLOGY, ACM JOURNAL OF EMERGING TECHNOLOGIES IN COMPUTING and several IEEE conferences.</p>
	<p><b>Santosh Khasanvis</b> received the B.Tech degree in electronics and communication engineering from Vellore Institute of Technology University, Vellore, India in 2008 and the M.S. degree in computer engineering from University of Massachusetts, Amherst, in 2012. He is currently working towards the Ph.D. degree in electrical and computer engineering at University of Massachusetts, Amherst.</p> <p>He is currently a Research Assistant with the Department of Electrical and Computer Engineering, University of Massachusetts, Amherst. His research interests include nanoscale computing</p>



	fabrics, machine learning, computer architecture and VLSI.
	<p><b>Csaba Andras Moritz</b> received the Ph.D. degree in computer systems from the Royal Institute of Technology, Stockholm, Sweden, in 1998. From 1997 to 2000, he was a Research Scientist with Laboratory for Computer Science, the Massachusetts Institute of Technology (MIT), Cambridge. He has consulted for several technology companies in Scandinavia and held industrial positions ranging from CEO, to CTO, and to founder. His most recent startup company, BlueRISC Inc, develops security microprocessors and hardware-assisted security solutions. His other project WindowsSCOPE focuses on cyber security tools. He is currently a Professor with the Department of Electrical and Computer Engineering, University of Massachusetts, Amherst. His research interests include nanoscale fabrics, post-CMOS nanoscale computing, computer architecture, and security.</p>